Microbiota Accessible Carbohydrates Facilitate Clearance of *Clostridium difficile*

Andrew J Hryckowian[1], William Van Treuren[1], Samuel A Smits[1], Nicole M Davis[1], Jackson O Gardner[1], Donna M Bouley[2], Justin L Sonnenburg[1]*

[1]Stanford University School of Medicine, Department of Microbiology and Immunology, Stanford, CA; [2]Stanford University School of Medicine, Department of Comparative Medicine, Stanford, CA

*Corresponding Author, jsonnenburg@stanford.edu

Clostridium difficile (*Cd*) is an opportunistic diarrheal pathogen and *Cd* infection (CDI) represents a major healthcare concern, causing an estimated 15,000 deaths per year in the United States alone[1]. Several enteric pathogens, including *Cd*, leverage inflammation and the accompanying microbial dysbiosis to thrive in the distal gut[2,3]. Although diet is among the most powerful available tools for affecting the health of humans and their relationship with their microbiota, investigation into the effects of diet on CDI has been limited. Here, we show in mice that the consumption of microbiota accessible carbohydrates (MACs) found in dietary plant polysaccharides has a significant impact on CDI. Specifically, using a murine model of antibiotic-induced CDI that typically resolves within 12 days of infection, we demonstrate that MAC-deficient diets perpetuate CDI. We show that *Cd* can be cleared through the addition of either a diet containing a complex mixture of MACs or a simplified diet containing inulin as the sole MAC source. We show that switches between these dietary conditions are coincident with changes to microbiota membership, its metabolic output and *Cd*-mediated inflammation. Together, our data demonstrate the outgrowth of MAC-utilizing taxa and the associated end products of MAC metabolism, namely the short chain fatty acids (SCFAs) acetate, propionate, and butyrate, are associated with decreased *Cd* fitness despite increased toxin production in the gut. Our findings, when placed into the context of the known fiber deficiencies of a human Western diet, suggest utility in microbiota-informed MAC-centric dietary strategies for the mitigation of CDI and other gastrointestinal infectious diseases.

The onset of CDI is typically associated with antibiotic-mediated dysbiosis, yet 22% of individuals with community acquired CDI have no recent history of antibiotic use[4]. The use of proton pump inhibitors, recent hospitalization, impaired immune function, advanced age, and diet may also provide dysbiotic conditions conducive to *Cd* fitness in the gut[5,6]. We and others previously demonstrated that direct microbiota-*Cd*

metabolic interactions are critical determinants of *Cd* fitness in the distal gut[7-9] and that the absence of dietary MACs leads to the expression of inflammatory markers by the host colonic epithelium[10]. One hypothesis is that MACs may positively affect CDI outcome by favoring a diverse microbiota[11,12]. Additional *in vitro* work suggested that MAC-centric metabolic interactions may play a role in reducing the fitness of *Cd* in the gut[13-15], leading us to hypothesize that a MAC-deficient diet reinforces a *Cd*-mediated inflammatory state.

We used an experimental model of CDI in ex-germ-free Swiss-Webster mice colonized with the microbiota of a healthy human donor (See Methods). These humanized mice were fed a diet containing a complex mixture of MACs (MAC^+), or two diets that differ substantially in fat content but are both MAC-deficient (MD) (**Fig. 1a**; see Methods for details of diet compositions). Groups of mice fed either MD diet show persistent CDI while mice fed the MAC^+ diet clear the pathogen below detection within 10 days of infection. After 36 days of persistent infection in mice fed the MD diets, a dietary shift to the MAC^+ diet results in clearance below detection within 9 days (**Fig. 1a**). This MAC^+ diet-mediated CDI clearance is also observed in conventional Swiss-Webster mice, in ex-germ-free Swiss-Webster mice colonized with a conventional Swiss-Webster mouse microbiota and in conventional C57BL/6 mice (**Fig. S1**), demonstrating that MAC-dependent CDI clearance is not confined to a specific microbiota or host genotype.

To enumerate gut-resident microbes that might participate in MAC-dependent CDI clearance, we sequenced 16S rRNA amplicons from the feces of humanized mice (**Fig. 1a**). The presence of dietary MACs and treatment with antibiotics affected both alpha and beta diversity of operational taxonomic units (OTUs) in the gut microbiota (**Figs. 1b-d**, **S2, S3**). Two principle coordinates could explain 48% of the variance in weighted UniFrac distances between samples, allowing us to visualize changes to overall community composition over time. We traced changes in the composition of the

92 microbiota over time and to highlight the composition of the microbiota in the context of
93 CDI, a log-fold contour plot was drawn to illustrate burdens of *Cd* that correspond to
94 these samples (see **Fig. S4** for further explanation of these "contoured PCoA" [cPCoA]
95 plots).

96 Following clindamycin treatment, the microbiota of all mice is remodeled to a *Cd*-
97 permissive state (**Figs. 1b-d**, dotted lines; **Fig. S3**). After inoculation with *Cd*, the
98 microbiota of MAC$^+$ fed mice changes significantly, and as CDI clearance occurs, the
99 community returns to resemble the pre-infection state (**Figs. 1b, S3a**), illustrating
100 compositional resilience of the microbiota under the MAC$^+$ *Cd* non-permissive dietary
101 condition. The microbiota of mice fed the MD diets also undergoes significant changes
102 during experimental CDI, however, during persistent infection, microbiota composition is
103 similar to the pre-infection microbiota associated with dietary MAC-deficiency. Upon
104 dietary intervention with MACs, the microbiota of these mice transitions to resemble the
105 microbiota of mice fed the MAC$^+$ diet as they clear *Cd* (**Figs. 1c, 1d, S3b, S3c**). These
106 data suggest that diet and antibiotic treatment are the dominant drivers of microbial
107 communities that support or exclude *Cd* in our model. Furthermore, the similarities in the
108 microbiota of uninfected and persistently infected mice fed the MD diets may be due to
109 the metabolic and compositional constraints imposed by this dietary condition, which we
110 hypothesize is supportive to *Cd* during infection.

111 Since limitation of dietary MACs is known to increase inflammation in the
112 gastrointestinal tract[10], we examined whether diet-induced inflammation impacted *Cd*
113 during persistence. Humanized Swiss-Webster mice fed the MD1 diet were infected as
114 in **Fig. 1a,** and after persistent CDI was established, were given the MAC$^+$ diet at 7 days
115 post infection. At pre- and post-diet shift time points, histopathology of proximal colon
116 tissue was evaluated. Inflammation was significantly increased in all infected mice
117 relative to uninfected control mice fed the MAC$^+$ diet, as illustrated by inflammatory cell

infiltrates into the submucosa and lamina propria of the colon (**Figs. 2a, S5; Table S1**). Notably, inflammation is comparably elevated in both infected and uninfected mice fed the MD1 diet, consistent with the contribution of the MD diets to inflammation and *Cd* persistence. Inflammation is most pronounced in infected mice that underwent the MD1 to MAC$^+$ diet shift (**Fig. 2a**), suggesting that *Cd* causes greater inflammation in gastrointestinal tracts that are non-permissive to *Cd* fitness.

We measured burdens of *Cd* and levels of a critical *Cd* virulence factor, the glycosylating toxin TcdB[16], in feces during the shift from a permissive to a non-permissive environment, specifically at 0, 2, and 4 days post MD1 to MAC$^+$ diet shift. TcdB is detected during persistent infection, and toxin expression is further elevated at 2 and 4 days after the shift to the clearance-mediating MAC$^+$ diet (**Fig. 2b,** 14.5-fold increase in cfu-normalized abundance from day 0 to day 2; $p<0.0001$ and 6.5-fold increase from day 0 to day 4; $p=0.0066$). Though cfu-normalized TcdB abundance is elevated after the diet shift, the overall abundance of TcdB decreases from day 2 to day 4 post diet shift (**Fig. S6**, 2.4-fold, $p=0.0086$). This shows that toxin expression is elevated on a per-cell basis in the MAC$^+$ environment, however overall TcdB abundance scales with decreasing burdens of *Cd* after a diet shift. The expression of TcdAB in *Cd* is controlled by multiple inputs, such as nutrient availability, quorum sensing, and other environmental stresses[17]. Together, these data demonstrate that a lack of dietary MACs facilitates a level of inflammation permissive to *Cd* survival in the gut, enabling persistence despite lower levels of toxin expression by *Cd*. The change to the *Cd*-inhospitable MAC$^+$ dietary condition is characterized by increased toxin expression and concomitant elevated inflammation.

In a previous report, in mice that cleared CDI below the limit of detection, high-level *Cd* shedding could be re-initiated upon clindamycin treatment up to approximately 12 weeks post FMT-mediated clearance[3], consistent with mice harboring *Cd* in the

absence of disease and not having developed protective immunity. In our model of MAC-mediated clearance of CDI, the persistently infected state cannot be re-established by switching cleared mice to the MD1 diet. However, persistent infection can be re-established if mice are first switched to the MD1 diet and treated with clindamycin (**Fig. S7**).

Having shown that the MAC$^+$ diet, containing a complex and ill-defined mixture of MACs (see Methods), is successful in clearing CDI, we sought to decouple the effects of MACs from other components that differ between our MAC$^+$ and MD diets (e.g. phytonutrient[18] or protein[12] content). Humanized mice whose CDI was reactivated with clindamycin treatment as in Fig. S7 (**Fig. 3a**) and mice that were *Cd*-naïve (**Fig. S8**) recapitulate findings from our dietary intervention experiment in mice using a simplified diet based on the MD1 diet containing inulin as the sole MAC source. We also demonstrate that prophylactic inulin feeding (either 10% in the diet as above or 1% in the drinking water of mice fed the MD1 diet), results in dose-dependent effects on both the maximum *Cd* burden and on *Cd* clearance kinetics (**Fig. S9**). Taken together, like the complex MAC$^+$ diet, inulin feeding results in significant reductions of *Cd* burdens across experimental paradigms (**Figs. 3a, S8-S10**).

Notably, 2 of 16 mice given inulin-based dietary interventions failed to clear *Cd* below detection (**Fig. S8a**). However, TcdB is not detectable in these mice (or the MAC$^+$-fed mice that cleared *Cd* below detection) at the endpoint of this experiment (**Fig. S8b**). Intuitively, CDI severity is correlated with fecal toxin level in adults[19], ranging from asymptomatic carriage to fulminant colitis (up to 15% of healthy adults are asymptomatically colonized with *Cd*[20]). However, *Cd* toxin levels are rarely quantified in current clinical diagnostic procedures[21]. This raises the possibility that MAC-mediated reduction of *Cd* burdens below a pathogenic threshold may be sufficient to mitigate disease in at-risk individuals.

Although the complex MAC$^+$ and the inulin containing diets both negatively impact the *in vivo* fitness of *Cd*, the overall community composition differs substantially between these two diets, as illustrated by a two-dimensional cPCoA subspace that explains 62% of the variation in the data **(Fig. 3b)** and the proportional abundance of taxa (**Figs. S11, S12**). Increased gut microbiota diversity is associated with resistance to a number of pathogens and is a hallmark of FMT-mediated CDI clearance[9,22-24]. We hypothesized the MAC rich diets might increase the diversity of the microbiota, thereby facilitating CDI clearance. Consistent with this hypothesis, the CDI clearance induced by the MAC$^+$ diet is correlated with an increase in alpha diversity of the gut microbiota ($p<0.0001$). However, alpha diversity does not increase when mice undergo inulin-mediated clearance, as measured by Shannon Diversity Index (**Figs. 3c, S13a**). We calculated the Gini Index, with higher scores indicating less evenness in community OTU composition. Community evenness is lowest in the inulin fed mice relative to mice fed either the MAC$^+$ or MD1 diet (**Fig. S13b**, $p<0.0001$), consistent with a limited number of taxa profiting directly from a single type of MAC[25]. In aggregate, we demonstrate that addition of a single MAC type (i.e. inulin) significantly reduces *Cd* burdens but that clearance does not depend upon an increase in microbiota diversity.

Despite these wholesale differences in community composition and alpha diversity, we pursued two of several possibilities: (1) a common subset of OTUs facilitates clearance across dietary interventions or (2) diet-specific but functionally similar OTUs within dietary conditions facilitate clearance. To identify taxonomic features that are predictive of *Cd* presence within or across dietary conditions or that discriminate between dietary conditions utilized in this study (**Table S2**, fields 'Plus_minus_Cd' and 'Current_diet,' respectively), we performed supervised (random forests) and unsupervised (non-parametric tests for differential abundance) analyses on OTUs identified in this study. These methods gave highly similar results: all of the features

identified by supervised analysis as the most discriminating between *Cd* infection state or diet for each comparison group (n=15 for each classifier) were also identified by unsupervised analysis (Bonferroni corrected p<0.05, **Table S3**). The correlation between these important features and *Cd* burdens was further explored by Spearman correlation analyses, refining a list of high-confidence taxa that are predictive of *Cd* burdens (Spearman ρ with Bonferroni corrected p<0.05, **Table S4**). Notably, several taxa are significantly (anti)correlated with *Cd* burdens regardless of diet, suggesting that common microbial signatures may underlie permissive and non-permissive states (**Table S4**). Among these, features corresponding to *Parabacteroides*, Lachnospiraceae, and Erysipelotrichaceae are significantly correlated with *Cd* abundance regardless of diet. Our observed correlation between *Parabacteroides* and levels of *Cd* is consistent with previous observations that members of this genus are consistently found in *Cd* "supershedder" mice[26]. In humans, Erysipelotrichaceae and some Lachnospiraceae are enriched in individuals with CDI compared to nondiarrheal controls[27]. Despite these commonalities among dietary conditions, the majority of the features identified in **Table S4** are only (anti)correlated with *Cd* in a subset of diets, supporting previous work from Schubert and colleagues that multiple distinct context-dependent communities, rather than core *Cd*-(un)supportive communities, are important for determining CDI status[28]. Others have demonstrated that metabolites, rather than microbes, are able to differentiate CDI status in humans[29] and that differences in antibiotic exposure can change the landscape of nutrients available to *Cd* during murine model CDI[30]. We therefore hypothesized that diet creates metabolic landscapes that are either supportive or unsupportive of *Cd*, and that the identification and manipulation of metabolites that characterize environments that are unsupportive of CDI will open new therapeutic avenues to mitigating CDI and other gastrointestinal infectious diseases.

Therefore, we pursued whether the inulin and MAC$^+$-mediated clearance conditions could be differentiated from the permissive condition on a molecular basis that is relevant to MAC metabolism. We measured the major metabolic end products of MAC metabolism (the SCFAs acetate, propionate, and butyrate) in cecal contents of mice shown in **Fig. S8** that were fed the MAC$^+$, inulin, and MD1 diets. Acetate and butyrate are both elevated in the ceca of mice fed MAC$^+$ and inulin diets relative to those fed the MD1 diet, and propionate is elevated in the ceca of MAC$^+$-fed mice relative to those fed the MD1 or inulin diets (**Fig. 4a).** We demonstrate that acetate, propionate, and butyrate have concentration-dependent negative effects on *Cd* growth, as measured by differences in doubling time (**Fig. 4b**). These findings using *Cd* strain 630 support previous findings that these SCFAs inhibit growth of four non-630 strains at concentrations as low as 20 mM[15].

Given these findings, we hypothesize that dietary MACs negatively affect the fitness of *Cd* in two interrelated ways. First, MACs drive privileged outgrowth of MAC-utilizing members of the microbiota (e.g. *Bacteroides* spp., see **Table S3b**). Second, the SCFAs that result from MAC metabolism negatively affect the fitness of *Cd*, which could be due to possibly due to the buildup of endproducts of key metabolic pathways, such as reductive acetogenesis and butyrogenesis[8,31].

Butyrate was previously shown to increase *Cd* toxin expression in *Cd* strain VPI 10463 in vitro[32]. Here, we demonstrate that acetate, propionate, and butyrate have concentration-dependent positive effects on TcdB expression in *Cd* strain 630 in vitro (**Fig. 4c**). Our findings are consistent with a model where SCFAs serve as a signal to *Cd* that the gut has become inhospitable. Whether SCFA-dependent *Cd*-mediated inflammation leads to the exclusion of inflammation-sensitive competitors or to the creation of privileged nutrients, analogous to strategies delineated for the enteric pathogen *Salmonella* Typhimurium, remain to be determined[33]. Importantly, in the

murine model described herein, the negative effects on *Cd* fitness engendered by the sustained consumption of MAC-rich diets override the ability of *Cd* to maintain or regain its niche in the gastrointestinal tract.

To date, microbiota-centric therapies for CDI, such as fecal microbiota transplant and probiotic administration, have focused on the introduction of exogenous organisms whose functionalities exclude *Cd* from the community. Our work shows that dietary intervention supports microbial communities that exclude *Cd* without the requirement for microbe introduction. Despite inter-experiment and inter-animal variations in clearance kinetics (**Fig. S10**), the effect is highly reproducible. Clearance kinetics may be further affected by host genetics, initial microbiota composition, or overall dietary MAC concentration/composition. Despite the individuality in the gut microbiota of patients with CDI, there is a consistent metabolic response that underlies CDI across individuals[29]. In light of observations that MACs profoundly alter the composition and function of the microbiota and host physiology[34,35], our findings raise the possibility that SCFAs, which are not easily measured in current shotgun metabolomics pipelines, are a critical part of the metabolic landscapes tied to CDI status across individuals. Advances in measuring these key reporters of community metabolism in the fecal matrix, or more proximally in the colon of humans will greatly advance understanding how diet shapes gut ecology.

Notably, two independent human trials have shown cooked green bananas (rich in MACs as evident by elevated SCFAs in the stool of treated patients) aid host recovery from another enteric pathogen, *Shigella*[36,37]. More recently, it was shown that a MAC-deficient diet leads to microbiota-dependent mucus degradation and attachment-dependent lethal colitis by the murine pathogen, *Citrobacter rodentium*[38]. Taken together, these observations suggest that further dissection of MAC-by-microbiota pathogen clearance mechanisms will be broadly applicable to many gastrointestinal infectious diseases. Our work provides evidence that dietary manipulation of the

metabolic networks of the intestinal tract offer a new lever to influence *Cd* and other gastrointestinal pathogens. These findings reveal an immediate need for simple, inexpensive, and safe diet-focused studies in appropriate human cohorts.

Methods

Media and bacterial growth conditions

Frozen stocks of *Clostridium difficile* (*Cd*) strain 630[39] were maintained under anaerobic conditions in septum-topped vials. *Cd* 630 was routinely cultured on CDMN agar, composed of *Cd* agar base (Oxoid) supplemented with 7% defibrinated horse blood (Lampire Biological Laboratories), 32 mg/L moxalactam (Santa Cruz Biotechnology), and 12 mg/L norfloxacin (Sigma-Aldrich) in an anaerobic chamber at 37˚ (Coy). After 16-24 hours of growth, a single colony was picked into 5 mL of pre-reduced Reinforced Clostridial medium (RCM, Oxoid) and grown for 16 hours. This 16-hour culture was used as the inoculum for murine model CDI, below.

For in vitro growth experiments, *Cd* 630 was cultured on CDMN as above. Single colonies were picked into pre-reduced *Cd* minimal medium (CDMM) without glucose, as described previously[40]. After 16 hours of growth, subcultures were prepared at a 1:200 dilution in pre-reduced CDMM supplemented with 0, 10, or 30 mM of sodium acetate (Fisher), sodium propionate (Sigma Aldrich), sodium butyrate (Sigma Aldrich), or sodium chloride (EMD Millipore) in sterile polystyrene 96 well tissue culture plates with low evaporation lids (Falcon). To further minimize evaporation of culture media during growth, the 36 wells along the perimeter of the 96 well plates were filled with water rather than culture. Cultures were grown anaerobically as above in a BioTek Powerwave plate reader and at 15-minute intervals, the plate was shaken on the ‘slow’ setting for 1 minute and the optical density (OD_{600}) of the cultures was measured and recorded using

298 Gen5 software (version 1.11.5). After 24 hours of growth, culture supernatants were
299 collected after centrifugation for 5 minutes at 2,500 x g and stored at -20˚C.
300
301 **Murine model CDI**
302 All animal studies were conducted in strict accordance with the Stanford
303 University Institutional Animal Care and Use Committee (IACUC) guidelines. Murine
304 model CDI was performed on age- and sex-matched mice between 8 and 17 weeks of
305 age, possessing one of three gut microbiota colonization states: (1) Humanized Swiss-
306 Webster mice: Germ free mice (SWGF, Taconic; bred in house) were inoculated with a
307 fecal sample obtained from a healthy anonymous donor, as used in previous studies
308 from our laboratory[41,42], (2) Conventionally-reared Swiss-Webster mice (SWRF, Taconic;
309 bred in house); or C57BL/6 mice (B6EF, Taconic; experiments conducted on animals
310 acquired directly from vendor), and (3) Conventionalized mice: Germ free Swiss-
311 Webster mice were inoculated with a fecal sample obtained from SWRF mice. The gut
312 microbial communities of the humanized and conventionalized mice were allowed to
313 engraft for at least 4 weeks, a period of time sufficient for community equilibration[43].
314 To initiate CDI, mice were given a single 1mg dose of clindamycin by oral gavage
315 (200 µL of a 5 mg/mL solution) and were infected 24 hours later with 200 µL of overnight
316 culture grown in RCM (approximately $1.5x10^7$ cfu/mL) or mock infected with 200 µL filter
317 sterilized PBS. To reactivate CDI in mice that had cleared the infection below detection,
318 mice were given a single dose of clindamycin by oral gavage as above.
319 Feces were collected from mice directly into microcentrifuge tubes and placed on
320 ice. To monitor *Cd* burdens in feces, 1 µL of each fecal sample was resuspended in PBS
321 to a final volume of 200 µL, 10-fold serial dilutions of fecal slurries (through 10^{-3}-fold)
322 were prepared in 96-well plates. For each sample, duplicate 10 µL aliquots of each
323 dilution were spread onto CDMN agar. After 16-24 hours of anaerobic growth at 37˚C

colonies were enumerated in duplicate spots were averaged to give cfu values. The limit of detection of this plating assay is $2x10^4$ cfu/mL feces. *Cd* was undetectable in all mice prior to inoculation with *Cd* (**Figs. 1A, S1, S8-S10**) and in all mice that were mock infected with PBS (**Fig. S8**), supporting that the animals used in this work were not pre-colonized with *Cd* (e.g. *Cd* LEM1, as seen by Etienne-Mesmin and colleagues[44]). After serial dilution of fecal samples, the remaining amounts of fecal samples were immediately frozen at -80˚C until needed for 16S rRNA analysis and measurement of TcdB via ELISA, below. It was not possible to blind researchers to infection or dietary status of the animals.

Mouse diets

Mice were fed one of four diets in this study ad libitum: (1) a diet containing a complex mixture of MACs (MAC^+, Purina LabDiet 5010); (2) a custom MAC-deficient diet[45] [MD1, 68% glucose (w/v), 18% protein (w/v), and 7% fat (w/v) (Bio-Serv); (3) a commercially available MAC-deficient diet [MD2, 34% sucrose (w/v), 17% protein (w/v), 21% fat (w/v); Harlan TD.88137], or (4) a custom diet containing inulin as the sole MAC source[45] [58% glucose (w/v); 10% inulin (w/v) [Beneo-Orafti group; OraftiHP]; 18% protein (w/v), and 7% fat (w/v) (Bio-Serv)]. Where applicable, the drinking water of mice fed the MD1 diet was supplemented with 1% inulin (w/v) [Beneo-Orafti group; OraftiHP]. Because mice consume approximately 5 grams of food per day and 5 mL of water per day[46], water with 1% inulin gives an approximate 10-fold reduction in inulin consumed relative to the 10% inulin diet. Groups of mice were randomly assigned to dietary conditions.

Histology and histopathological scoring

Proximal colon sections harvested for histopathologic analyses were fixed in 10% buffered neutral formalin and routinely processed for paraffin embedding, sectioned at 4 microns, mounted on glass slides and stained with hematoxylin and eosin (Histo-tec Laboratory, Hayward, CA). Analyses were performed by a board certified veterinary pathologist, using a semiquantitative scoring system[47] that evaluated distribution and severity of cellular infiltrates (inflammation) using a severity score of 0 to 5 (0 = no significant lesion, 1 = minimal, 2 = mild, 3 = moderate, 4 = marked, 5 = severe).

Quantification of *C. difficile* toxin TcdB

Levels of TcdB in feces and culture supernatants were measured using the "Separate detection of *C. difficile* toxins A and B" kit (TGC Biomics) according to the manufacturer's instructions. For each fecal sample, toxin abundance was normalized by the number colony forming units, as determined by selective culture on CDMN agar (above), for each sample; "Normalized TcdB Abundance in Feces" = [(x ng toxin) / (y cfu *C. difficile* mL^{-1} feces)] and is reported in **Fig. 2b**. Non-normalized TcdB abundance in mouse feces is reported in **Fig. S6**. For culture supernatants, toxin abundance was normalized by the final OD_{600} of the culture and "Normalized TcdB Abundance in Culture Supernatant" = [(x ng toxin) / (y OD600)] and is reported in **Fig. 4c**.

16S rRNA amplicon sequencing and OTU picking methods

Total DNA was extracted from frozen fecal material using the PowerSoil DNA Isolation Kit (MoBio) or the Powersoil-htp 96 well DNA isolation kit (MoBio). Barcoded primers were used to amplify the V3-V4 region of the 16S rRNA gene from extracted bacterial DNA using primers 515f and 806rB via PCR[48]. Following amplicon cleanup using the UltraClean PCR Clean-Up Kit (MoBio) and quantification using the high sensitivity Quant-iT dsDNA Assay Kit (Thermo Fisher). Amplicons were pooled to an

equimolar ratio. 16S rRNA amplicons from 3 mouse experiments were sequenced in 3 different paired-end Illumina MiSeq runs, with each experiment occurring on a separate run. The sample split/run corresponds to the field 'Experiment' in **Table S2**.

For exact commands executed for the 16S rRNA-based bioinformatics analysis, please see **Code S1**, an ipython notebook that records commands and code used. Runs were demultiplexed independently due to some non-unique barcodes, and then concatenated prior to OTU picking using 'split_libraries_fastq.py' with default quality parameters in QIIME 1.9.1[49]. Open reference OTU picking was conducted with default parameters using the QIIME script 'pick_open_reference_otus.py' (with default clustering algorithm UCLUST[50]) on the 24,582,127 reads that passed quality filtering. OTUs whose representative sequence failed to align to the Greengenes reference alignment with at 85% identity using PyNAST were discarded[51,52].

We removed OTUs occuring in at least 10 samples, and/or having less than 26 counts in the entire dataset. This filtering reduced the number of OTUs by 95.04% (211,884 to 10,504) but removed only 5.2% of the feature-mass (23,293,178 to 22,078,743). This type of filtering removes a vast number of features that are likely artefacts, boosts power by reducing false discovery penalties, and concentrates analysis on biologically meaningful features. We rarefied our data to correct for differences sequencing depth. To ensure our results were not artefacts of rarefaction depth we conducted analyses at multiple rarefaction levels and our conclusions were not changed. We use OTU tables rarefied to 7,000 in this study, facilitating inter-run comparisons.

Supervised learning

Using the 'supervised_learning.py' script from QIIME 1.9.1, the random forests classification method (with 10-fold cross validation error estimation) was trained using an OTU table as prepared above in "16S sequencing and OTU picking methods." Presence

or absence of *Cd* in a fecal sample (as determined by selective culture) or current diet were used as the class label category, corresponding to the field 'Plus_minus_Cd' and 'Current_diet' of **Table S2**. The OTU table was modified for this analysis by querying each of the 11 *Cd* 630 rRNA sequences against a BLAST database built from the representative set of OTUs created during OTU picking (see "16S sequencing and OTU picking methods"), after which the OTUs that matched *Cd* 630 rRNA sequences (cutoff 97% identity) were collapsed into a single *Cd* OTU, "k__Bacteria;p__Frimicutes;c__Clostridia;o__Clostridiales;f__Peptostreptococcaceae;g__Clostridioides;s__putative_difficile." See **Code S1** for the code used for this analysis.

Quantification of short chain fatty acids (SCFAs)

Immediately following euthanasia, cecal contents were removed from mice described in **Fig. S8**, weighed, and flash frozen in liquid nitrogen. Cecal contents (70-150 mg) were suspended in a final volume of 600 µl in ice-cold ultra pure water and blended with a pellet pestle (Kimble Chase) on ice. The cecal slurry was centrifuged at 2,350 x g for 30 seconds at 4˚C and 250 µL of the supernatant was removed to a septum-topped glass vial and acidified with 20µL HPLC grade 37% HCl (Sigma Aldrich). Diethyl ether (500 µL) was added to the acidified cecal supernatant to extract SCFAs. Samples were then vortexed at 4˚C for 20 minutes on 'high' and then were centrifuged at 1,000 x g for 3 minutes. The organic phase was removed into a fresh septum-topped vial and placed on ice. Then, a second extraction was performed with diethyl ether as above. The first and second extractions were combined for each sample and 250 µL of this combined solution was added to a 300 µL glass insert in a fresh glass septum-topped vial containing and the SCFAs were derivitized using 25 µL N-tert-butyldimethylsilyl-N-methyltrifluoroacetamide (MTBSTFA; Sigma Aldrich) at 60˚C for 30 minutes.

Analyses were carried out using an Agilent 7890/5975 single quadrupole GC/MS. Using a 7683B autosampler, 1 µL split injections (1:100) were made onto a DB-5MSUI capillary column (30 m length, 0.25 mm ID, 0.25 µm film thickness; Agilent) using helium as the carrier gas (1 mL/minute, constant flow mode). Inlet temperature was 200˚C and transfer line temperature was 300˚C. GC temperature was held at 60˚C for 2 minutes, ramped at 40˚C/min to 160˚C, then ramped at 80˚/min to 320˚C and held for 2 minutes; total run time was 8.5 minutes. The mass spectrometer used electron ionization (70eV) and scan range was m/z 50-400, with a 3.75-minute solvent delay. Acetate, propionate, and butyrate standards (20mM, 2mM, 0.2mM, 0.02mM, 0mM) were acidified, extracted, and derivatized as above, were included in each run, and were used to generate standard curves to enable SCFA quantification.

Measurement of doubling time for in vitro growth experiments

Raw OD_{600} measurements of cultures grown in CDMM (see "Media and bacterial growth conditions," above) were exported from Gen5 to MATLAB and analyzed using the growth_curve_analysis_v2_SCFA.m script and analyze_growth_curve_SCFA.m function (**Code S2** and **Code S3**, respectively). Growth rates were determined for each culture by calculating the derivative of natural log-transformed OD_{600} measurements with respect to time. Growth rate values at each time point were then smoothed using a moving average over 75-minute intervals to minimize artefacts due to noise in OD measurement data. To mitigate any remaining issues with noise in growth rate values, all growth rate curves were also inspected manually. Specifically, in cases where the analyze_growth_curve_SCFA function selected an artefactual maximum growth rate, the largest local maximum that did not correspond to noise was manually assigned as the maximum growth rate. Doubling time was then computed by dividing the natural log of 2

by maximum growth rate. The investigator that conducted growth curve analysis was blinded to the experimental conditions in which growth curve data were obtained.

Statistical methods

Alpha and beta diversity, correlations, and random forests were computed using QIIME ('alpha_diversity_through_plots.py', 'beta_diversity_through_plots.py', 'observation_metadata_correlations.py', 'supervised_learning.py'). Kruskal-Wallis, Mann-Whitey, Student's T, ANOVA, and D'Agostino-Pearson tests were performed using standard statistical analyses embedded in the Prism 7 software package (GraphPad Software Inc.). Spearman correlations were calculated in Python using **Code S1** under the heading 'feature correlations by diet'. Specific statistical tests are noted in figure legends or tables as applicable.

Data availability

The 16S sequence data have been uploaded to Qiita (http://qiita.ucsd.edu; Study ID 11347).

Code availability

For custom code used in this study, see **Code S1-S3**.

Acknowledgements

We thank Steven K. Higginbottom (Department of Microbiology and Immunology, Stanford) for expertise and technical assistance in all mouse experiments, Allis S. Chien (Stanford University Mass Spectrometry Facility) for developing the GC-MS parameters used in this study, and Carlos G. Gonzalez (Department of Chemical and Systems Biology, Stanford) for assistance with DNA extractions from mouse feces. This work was

477 funded by a grant from National Institutes of Health NIDDK (R01-DK085025 to J.L.S.),
478 an NIH postdoctoral NRSA (5T32AI007328 to A.J.H.), a Stanford University School of
479 Medicine Dean's Postdoctoral Fellowship (A.J.H.), NSF Graduate Research Fellowships
480 (S.A.S, W.V.T - DGE-114747), an NIH predoctoral NRSA (5T32AI007328 to N.M.D.),
481 and a Smith Stanford Graduate Fellowship (S.A.S.). J.L.S. received an Investigators in
482 the Pathogenesis of Infectious Disease Award from the Burroughs Wellcome Fund.

483

484 **Author Contributions**

485 A.J.H., N.M.D., and J.O.G. performed the experiments. D.M.B. conducted blinded
486 scoring, imaging, and analysis of tissue sections. A.J.H., W.V.T., S.A.S., N.M.D.,
487 D.M.B., and J.L.S. analyzed and interpreted data, designed experiments, and prepared
488 display items. A.J.H. and J.L.S. wrote the paper. All authors edited the manuscript prior
489 to submission.

490

491 **Competing interests**

492 The authors declare no competing interests.

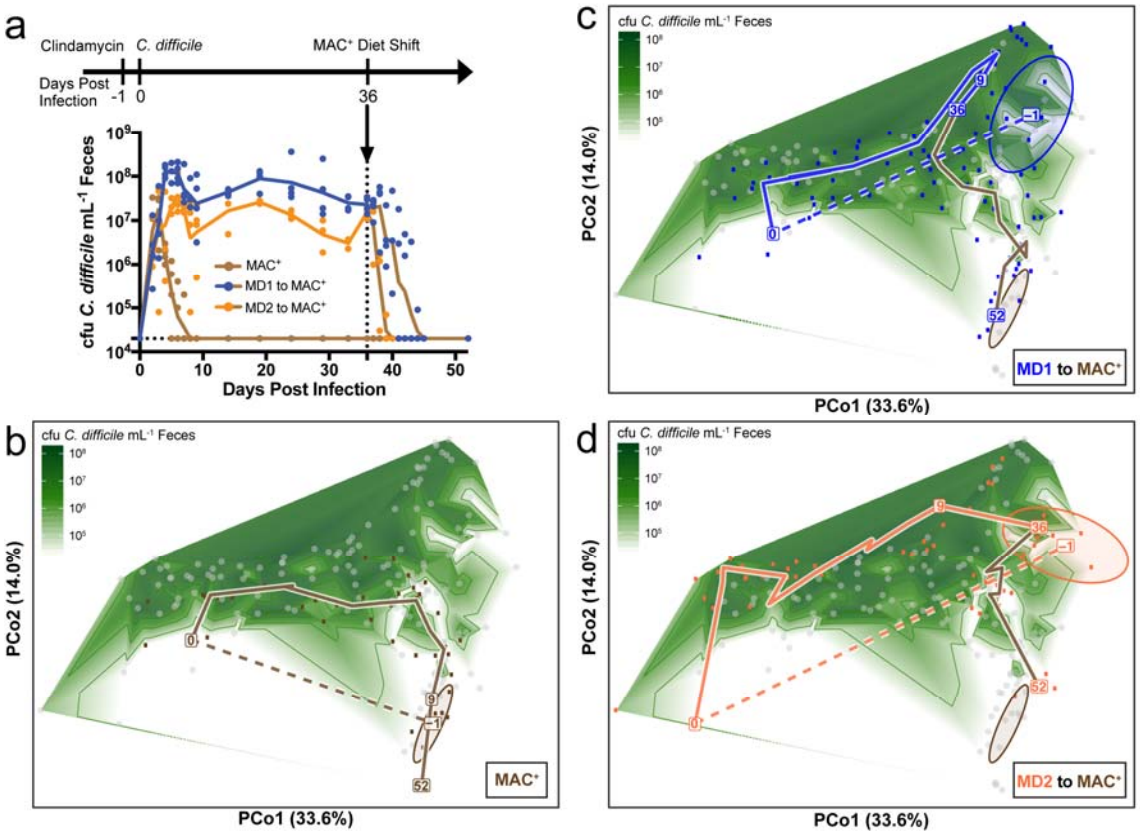

493

494 **Figure 1. Dietary MACs toggle the fitness of *Clostridium difficile* (*Cd*) in the gut**

495 **while engendering distinct microbiota states.** Humanized, age matched female

496 Swiss-Webster mice were maintained on a diet containing a complex mixture of MACs

497 (MAC$^+$, n=4 mice) or on diets deficient in MACs (MD1, n=4 mice; and MD2, n=4 mice)

498 starting 8 days pre-infection. **(a)** All mice were subsequently subjected to murine model

499 CDI and were gavaged with clindamycin at 1 day before infection with *Cd*. At 36 days

500 post-infection, mice fed the MD diets were switched to the MAC$^+$ diet. Burdens of *Cd*

501 were monitored over time by selective culture, as described in Methods. One of the MD2

502 fed mice was moribund on D10 and was euthanized. Individual per-sample *Cd* burdens

503 are plotted and lines represent geometric mean burdens per time point. **(b-d)** Principal

504 coordinates analysis plots of Weighted UniFrac distances between microbiota samples

505 collected from these mice were prepared and overlaid with log-fold contour plots of *Cd*

506 burdens, as measured in panel A. Under all dietary conditions, clindamycin affects the

composition of the microbiota in all groups of mice from D-1 (annotated with ellipses representing 80% CI) to D0 (dotted lines), resulting in a dysbiotic state permissive to CDI. In each panel, a line is drawn through the centroid of the points for a given experiment day. **(c)** In mice fed the MAC^+ diet, the microbiota returns to resemble the pre-infection state as *Cd* clearance occurs. **(d, e)** In mice fed the MD1 and MD2 diets, respectively, CDI remains unresolved until dietary intervention with the MAC^+ diet at D36, which shifts the microbiota to resemble that of other MAC^+ fed mice as *Cd* clearance occurs (brown lines). Points are colored by the highlighted treatment group, or alternatively are retained as gray points for reference. See **Fig. S4** for further explanation on how to interpret the contoured PCoA (cPCoA) plots shown in panels b-d.

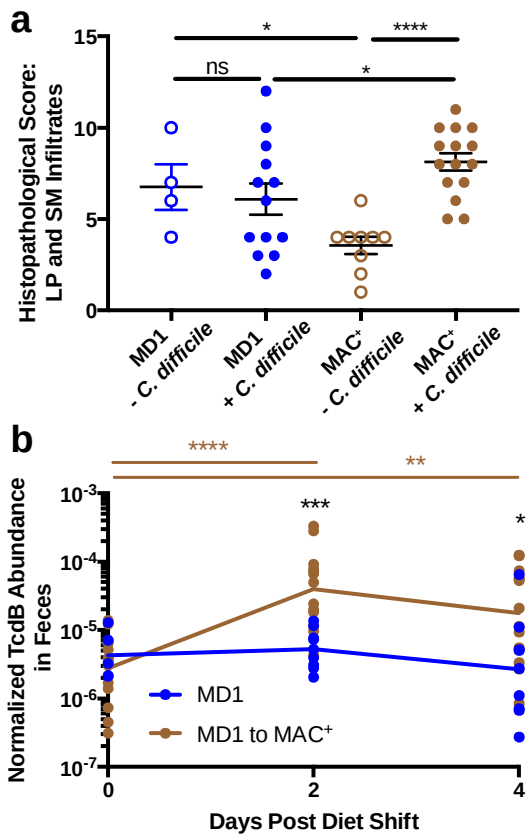

Figure 2. Inflammation and *Cd* toxin expression are diet-dependent. Age-matched, female, humanized Swiss-Webster mice were fed the MD1 diet, gavaged with clindamycin, and subsequently infected with *Cd* as in **Fig. 1** or were mock infected with filter sterilized PBS. After 7 days of infection, mice were switched to a diet containing a complex mixture of MACs (MAC^+) to induce clearance. **(a)** Mice were euthanized before and after diet change, at time points specified in **Table S1**. Histopathology was carried out on proximal colon tissue from these mice as described in Methods (n=4 for mock-infected mice fed the MD1 diet, n=9 for mock-infected mice fed the MAC^+ diet, n=13 for infected mice fed the MD1 diet, and n=15 for infected mice fed the MAC^+ diet). Statistical significance between groups was assessed by one-way ANOVA and Tukey's multiple comparison test (*= $p<0.05$; ****=$p<0.0001$). **(b)** For infected mice where >5 mg fecal material could be collected (n=14, n=13, and n=13 for mice at 0, 2, and 4 days post MD1

535 to MAC$^+$ diet shift, and n=5, n=9, and n=9 at matched time points for mice that were
536 maintained on the MD1 diet), levels of TcdB in the feces were measured and normalized
537 to the burdens of *Cd* detected. Points represent normalized toxin abundance for
538 individual fecal samples lines are drawn through the per-day per-diet geometric mean
539 normalized toxin abundance. Statistical significance between relevant pairs of treatment
540 groups was assessed by Mann-Whitney test (*= p<0.05; **= p<0.01; ***= p<0.001;
541 ****=p<0.0001).
542
543
544
545
546
547
548
549
550
551
552
553
554
555
556

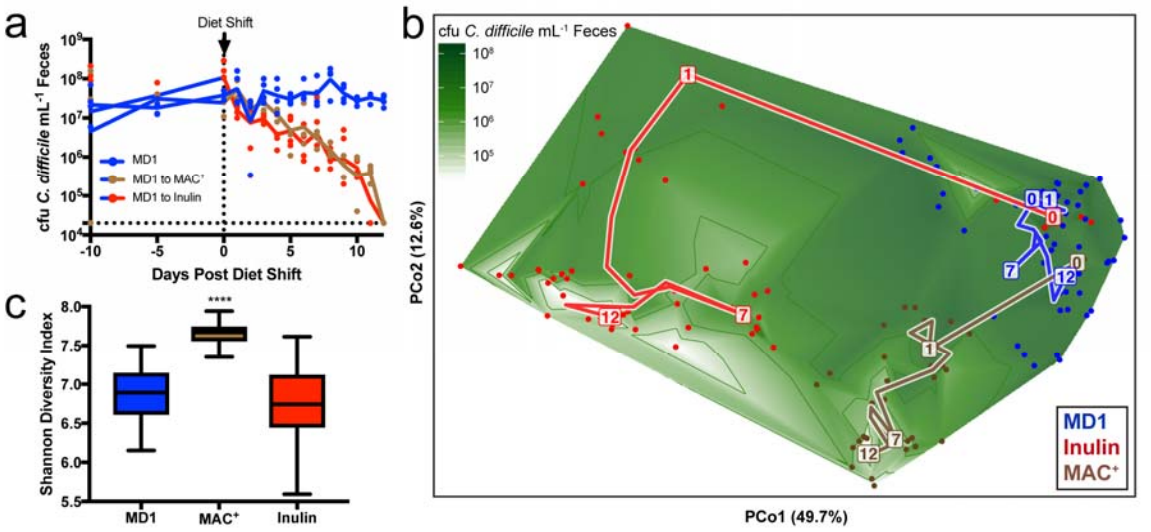

Figure 3. A diet containing inulin as the sole MAC source recapitulates the CDI clearance phenotype without increasing microbial diversity. Mice with persistent CDI were subjected to a dietary intervention of the complex MAC^{+} diet (n=3), a diet containing inulin as the sole MAC source (n=4), or were maintained on the MD1 diet (n=4). **(a)** Burdens of *Cd* were monitored over time by selective culture as described in Methods. Individual per-sample *Cd* burdens are plotted and lines represent geometric mean burdens per time point. **(b)** Contoured PCoA (cPCoA) plot of weighted UniFrac distances between microbiota samples collected from these mice was prepared and overlaid with log-fold contour plots of *Cd* burdens, as measured in panel A. A line is drawn through the centroid of the points for a given experimental day. See **Fig. S4** for further explanation on how to interpret cPCoA plots. **(c)** Alpha diversity of communities was determined longitudinally for the microbiota of these mice by Shannon Diversity Index. Differences in *Cd* burdens and alpha diversity between dietary conditions was determined by collapsing all post-intervention time points (See **Fig. S13** for temporal differences in Shannon Diversity Index). Statistical significance was determined by Kruskal Wallis test with Dunn's multiple comparison test (****= p<0.0001).

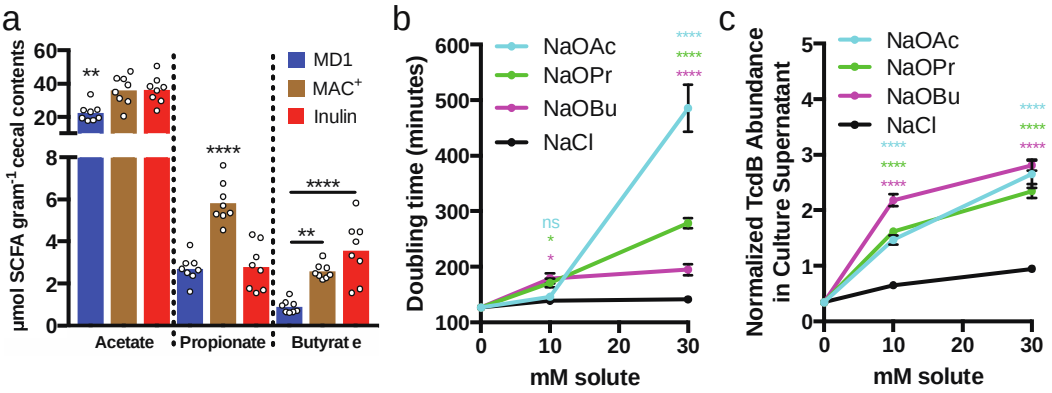

Figure 4. Acetate, propionate, and butyrate are elevated in the ceca of mice fed MACs, and affect growth and toxin production in *C. difficile.* (a) The short chain fatty acids acetate, propionate, and butyrate were measured in cecal contents of mice (n=8 per dietary condition) fed the MD1, MAC^{+}, and inulin containing diets (See **Fig S8** for time points of sacrifice corresponding to measurements). Data points represent per sample concentration of each SCFA and bars are drawn to represent the mean per-diet SCFA concentration. Statistical significance was assessed by ordinary one-way ANOVA and Tukey's multiple comparison test. (**, p<0.01; ****, p<0.0001) **(b)** Doubling time was calculated for *Cd* grown in CDMM supplemented with 0, 10, and 30 mM sodium acetate (NaOAc), sodium propionate (NaOPr), sodium butyrate (NaOBu), or sodium chloride (NaCl, sodium matched controls) as described in Methods. For each growth condition, at least n=16 independent cultures were assessed. **(c)** TcdB was quantified in supernatants from n=12 independent cultures from each growth condition as described in Methods. Points represent mean values, error bars represent ±SEM (panels b-d). Statistical significance (panels b-d) was assessed for each SCFA and sodium matched controls at each concentration via Mann-Whitney test (ns, not significant; *, p<0.05; ****, p<0.0001).

References

1 Lessa, F. C., Winston, L. G. & McDonald, L. C. Burden of *Clostridium difficile* infection in the United States. *The New England Journal of Medicine* **372**, 2369-2370, doi:10.1056/NEJMc1505190 (2015).

2 Ferreyra, J. A., Ng, K. M. & Sonnenburg, J. L. The Enteric Two-Step: nutritional strategies of bacterial pathogens within the gut. *Cellular Microbiology* **16**, 993-1003, doi:10.1111/cmi.12300 (2014).

3 Lawley, T. D. *et al.* Antibiotic treatment of *Clostridium difficile* carrier mice triggers a supershedder state, spore-mediated transmission, and severe disease in immunocompromised hosts. *Infection and Immunity* **77**, 3661-3669, doi:10.1128/iai.00558-09 (2009).

4 Khanna, S. *et al.* The epidemiology of community-acquired *Clostridium difficile* infection: a population-based study. *The American Journal of Gastroenterology* **107**, 89-95, doi:10.1038/ajg.2011.398 (2012).

5 Johnson, S. & Gerding, D. N. *Clostridium difficile*--associated diarrhea. *Clinical Infectious Diseases* **26**, 1027-1034; quiz 1035-1026 (1998).

6 Bignardi, G. E. Risk factors for *Clostridium difficile* infection. *The Journal of Hospital Infection* **40**, 1-15 (1998).

7 Ng, K. M. *et al.* Microbiota-liberated host sugars facilitate post-antibiotic expansion of enteric pathogens. *Nature* **502**, 96-99, doi:10.1038/nature12503 (2013).

8 Ferreyra, J. A. *et al.* Gut Microbiota-Produced Succinate Promotes *C. difficile* Infection after Antibiotic Treatment or Motility Disturbance. *Cell Host & Microbe* **16,** 770-777 (2014).

9 Buffie, C. G. *et al.* Precision microbiome reconstitution restores bile acid mediated resistance to *Clostridium difficile*. *Nature*, doi:10.1038/nature13828 (2014).

10 Earle, K. A. *et al.* Quantitative Imaging of Gut Microbiota Spatial Organization. *Cell Host & Microbe* **18**, 478-488, doi:10.1016/j.chom.2015.09.002 (2015).

11 Iizuka, M. *et al.* Elemental diet modulates the growth of *Clostridium difficile* in the gut flora. *Alimentary Pharmacology & Therapeutics* **20 Suppl 1**, 151-157, doi:10.1111/j.1365-2036.2004.01969.x (2004).

12 Moore, J. H. *et al.* Defined Nutrient Diets Alter Susceptibility to *Clostridium difficile* Associated Disease in a Murine Model. *PloS One* **10**, e0131829, doi:10.1371/journal.pone.0131829 (2015).

13 Hopkins, M. J. & Macfarlane, G. T. Nondigestible oligosaccharides enhance bacterial colonization resistance against *Clostridium difficile* in vitro. *Applied and Environmental Microbiology* **69**, 1920-1927 (2003).

14 Valdes-Varela, L., Hernandez-Barranco, A. M., Ruas-Madiedo, P. & Gueimonde, M. Effect of Bifidobacterium upon *Clostridium difficile* Growth and Toxicity When Co-cultured in Different Prebiotic Substrates. *Frontiers in Microbiology* **7**, 738, doi:10.3389/fmicb.2016.00738 (2016).

15 Kondepudi, K. K., Ambalam, P., Nilsson, I., Wadstrom, T. & Ljungh, A. Prebiotic-non-digestible oligosaccharides preference of probiotic bifidobacteria and antimicrobial activity against *Clostridium difficile. Anaerobe* **18**, 489-497, doi:10.1016/j.anaerobe.2012.08.005 (2012).

16 Lyras, D. *et al.* Toxin B is essential for virulence of *Clostridium difficile*. *Nature* **458**, 1176-1179, doi:10.1038/nature07822 (2009).

17 Martin-Verstraete, I., Peltier, J. & Dupuy, B. The Regulatory Networks That Control *Clostridium difficile* Toxin Synthesis. *Toxins* **8**, doi:10.3390/toxins8050153 (2016).

18 Wlodarska, M., Willing, B. P., Bravo, D. M. & Finlay, B. B. Phytonutrient diet supplementation promotes beneficial Clostridia species and intestinal mucus secretion resulting in protection against enteric infection. *Scientific Reports* **5**, 9253, doi:10.1038/srep09253 (2015).

19 Huang, B. *et al.* Real-time cellular analysis coupled with a specimen enrichment accurately detects and quantifies *Clostridium difficile* toxins in stool. *Journal of Clinical Microbiology* **52**, 1105-1111, doi:10.1128/jcm.02601-13 (2014).

20 Furuya-Kanamori, L. *et al.* Asymptomatic *Clostridium difficile* colonization: epidemiology and clinical implications. *BMC Infectious Diseases* **15**, 516, doi:10.1186/s12879-015-1258-4 (2015).

21 Pollock, N. R. Ultrasensitive Detection and Quantification of Toxins for Optimized Diagnosis of *Clostridium difficile* Infection. *Journal of Clinical Microbiology* **54**, 259-264, doi:10.1128/jcm.02419-15 (2016).

22 Kampmann, C., Dicksved, J., Engstrand, L. & Rautelin, H. Composition of human faecal microbiota in resistance to *Campylobacter* infection. *Clin Microbiol Infect* **22**, 61 e61-68, doi:10.1016/j.cmi.2015.09.004 (2016).

23 Ferreira, R. B. *et al.* The intestinal microbiota plays a role in *Salmonella*-induced colitis independent of pathogen colonization. *PloS One* **6**, e20338, doi:10.1371/journal.pone.0020338 (2011).

24 Seekatz, A. M. *et al.* Recovery of the gut microbiome following fecal microbiota transplantation. *mBio* **5**, e00893-00814, doi:10.1128/mBio.00893-14 (2014).

25 Walker, A. W. *et al.* Dominant and diet-responsive groups of bacteria within the human colonic microbiota. *The ISME journal* **5**, 220-230, doi:10.1038/ismej.2010.118 (2011).

26 Lawley, T. D. *et al.* Targeted restoration of the intestinal microbiota with a simple, defined bacteriotherapy resolves relapsing *Clostridium difficile* disease in mice. *PLoS Pathogens* **8**, e1002995, doi:10.1371/journal.ppat.1002995 (2012).

27 Schubert, A. M. *et al.* Microbiome data distinguish patients with *Clostridium difficile* infection and non-*C. difficile*-associated diarrhea from healthy controls. *mBio* **5**, e01021-01014, doi:10.1128/mBio.01021-14 (2014).

28 Schubert, A. M., Sinani, H. & Schloss, P. D. Antibiotic-Induced Alterations of the Murine Gut Microbiota and Subsequent Effects on Colonization Resistance against *Clostridium difficile*. *mBio* **6**, e00974, doi:10.1128/mBio.00974-15 (2015).

29 Rojo, D. *et al. Clostridium difficile* heterogeneously impacts intestinal community architecture but drives stable metabolome responses. *The ISME Journal* **9**, 2206-2220, doi:10.1038/ismej.2015.32 (2015).

30 Jenior, M. L., Leslie, J. L., Young, V. B. & Schloss, P. D. *Clostridium difficile* Colonizes Alternative Nutrient Niches during Infection across Distinct Murine Gut Microbiomes. *mSystems* **2**, doi:10.1128/mSystems.00063-17 (2017).

31 Kopke, M., Straub, M. & Durre, P. *Clostridium difficile* is an autotrophic bacterial pathogen. *PloS One* **8**, e62157, doi:10.1371/journal.pone.0062157 (2013).

32 Karlsson, S., Lindberg, A., Norin, E., Burman, L. G. & Akerlund, T. Toxins, butyric acid, and other short-chain fatty acids are coordinately expressed and down-regulated by cysteine in *Clostridium difficile*. *Infection and Immunity* **68**, 5881-5888 (2000).

33 Hryckowian, A. J., Pruss, K. M. & Sonnenburg, J. L. The emerging metabolic view of *Clostridium difficile* pathogenesis. *Current Opinion in Microbiology* **35**, 42-47, doi:10.1016/j.mib.2016.11.006 (2017).

34 Sonnenburg, E. D. & Sonnenburg, J. L. Starving our microbial self: the deleterious consequences of a diet deficient in microbiota-accessible carbohydrates. *Cell Metabolism* **20**, 779-786, doi:10.1016/j.cmet.2014.07.003 (2014).

35 Carmody, R. N. *et al.* Diet dominates host genotype in shaping the murine gut microbiota. *Cell Host & Microbe* **17**, 72-84, doi:10.1016/j.chom.2014.11.010 (2015).

36 Rabbani, G. H. *et al.* Green banana reduces clinical severity of childhood shigellosis: a double-blind, randomized, controlled clinical trial. *The Pediatric infectious disease journal* **28**, 420-425, doi:10.1097/INF.0b013e31819510b5 (2009).

37 Alvarez-Acosta, T. *et al.* Beneficial role of green plantain [*Musa paradisiaca*] in the management of persistent diarrhea: a prospective randomized trial. *Journal of the American College of Nutrition* **28**, 169-176 (2009).

38 Desai, M. S. *et al.* A Dietary Fiber-Deprived Gut Microbiota Degrades the Colonic Mucus Barrier and Enhances Pathogen Susceptibility. *Cell* **167**, 1339-1353 e1321, doi:10.1016/j.cell.2016.10.043 (2016).

39 Sebaihia, M. *et al.* The multidrug-resistant human pathogen *Clostridium difficile* has a highly mobile, mosaic genome. *Nature Genetics* **38**, 779-786, doi:10.1038/ng1830 (2006).

40 Cartman, S. T. & Minton, N. P. A mariner-based transposon system for in vivo random mutagenesis of *Clostridium difficile*. *Applied and Environmental Microbiology* **76**, 1103-1109, doi:10.1128/aem.02525-09 (2010).

41 Kashyap, P. C. *et al.* Complex interactions among diet, gastrointestinal transit, and gut microbiota in humanized mice. *Gastroenterology* **144**, 967-977, doi:10.1053/j.gastro.2013.01.047 (2013).

42 Sonnenburg, E. D. *et al.* Diet-induced extinctions in the gut microbiota compound over generations. *Nature* **529**, 212-215, doi:10.1038/nature16504 (2016).

43 Turnbaugh, P. J. *et al.* The effect of diet on the human gut microbiome: a metagenomic analysis in humanized gnotobiotic mice. *Science Translational Medicine* **1**, 6ra14, doi:10.1126/scitranslmed.3000322 (2009).

44 Etienne-Mesmin, L. *et al.* Toxin-positive *Clostridium difficile* latently infect mouse colonies and protect against highly pathogenic *C. difficile. Gut*, doi:10.1136/gutjnl-2016-313510 (2017).

45 Sonnenburg, E. D. *et al.* Specificity of polysaccharide use in intestinal bacteroides species determines diet-induced microbiota alterations. *Cell* **141**, 1241-1252 (2010)

46 Bachmanov, A. A., Reed, D. R., Beauchamp, G. K. & Tordoff, M. G. Food intake, water intake, and drinking spout side preference of 28 mouse strains. *Behavior Genetics* **32**, 435-443 (2002).

47 Gopinath, S., Lichtman, J. S., Bouley, D. M., Elias, J. E. & Monack, D. M. Role of disease-associated tolerance in infectious superspreaders. *Proceedings of the National Academy of Sciences of the United States of America* **111**, 15780-15785, doi:10.1073/pnas.1409968111 (2014).

48 Caporaso, J. G. *et al.* Ultra-high-throughput microbial community analysis on the Illumina HiSeq and MiSeq platforms. *The ISME Journal* **6**, 1621-1624, doi:10.1038/ismej.2012.8 (2012).

49 Caporaso, J. G. *et al.* QIIME allows analysis of high-throughput community sequencing data. *Nature Methods* **7**, 335-336, doi:10.1038/nmeth.f.303 (2010).

50 Edgar, R. C. Search and clustering orders of magnitude faster than BLAST. *Bioinformatics* **26**, 2460-2461, doi:10.1093/bioinformatics/btq461 (2010).

745 51 Caporaso, J. G. *et al.* PyNAST: a flexible tool for aligning sequences to a
746 template alignment. *Bioinformatics* **26**, 266-267,
747 doi:10.1093/bioinformatics/btp636 (2010).
748 52 McDonald, D. *et al.* An improved Greengenes taxonomy with explicit ranks for
749 ecological and evolutionary analyses of bacteria and archaea. *The ISME Journal*
750 **6**, 610-618, doi:10.1038/ismej.2011.139 (2012).
751